^{31}P NMR Saturation-Transfer and ^{13}C NMR Kinetic Studies of Glycolytic Regulation during Anaerobic and Aerobic Glycolysis†

S. L. Campbell-Burk,* J. A. den Hollander,‡ J. R. Alger, and R. G. Shulman

Department of Molecular Biophysics and Biochemistry and Department of Chemistry, Yale University, New Haven, Connecticut 06511

Received October 15, 1986; Revised Manuscript Received May 18, 1987

ABSTRACT: ^{31}P NMR saturation-transfer techniques have been employed in glucose-grown derepressed yeast to determine unidirectional fluxes in the upper part of the Embden–Meyerhof–Parnas pathway. The experiments were performed during anaerobic and aerobic glycolysis by saturating the ATP_γ resonances and monitoring changes in the phosphomonoester signals from glucose 6-phosphate and fructose 1,6-bisphosphate. These experiments were supplemented with ^{13}C NMR measurements of glucose utilization rates and ^{13}C NMR label distribution studies. Combined with data obtained previously from radioisotope measurements, these ^{31}P and ^{13}C NMR kinetic studies allowed estimation of the net glycolytic flow in addition to relative flows through phosphofructokinase (PFK) and Fru-1,6-P_2ase during anaerobic and aerobic glycolysis. The ^{31}P NMR saturation-transfer results are consistent with previous results obtained from measurements of metabolite levels, radioisotope data, and ^{13}C NMR studies [den Hollander, J. A., Ugurbil, K., Brown, T. R., Bednar, M., Redfield, C., & Shulman, R. G. (1986a) *Biochemistry 25*, 203–211], providing additional support for in vivo measurement of the flows during glycolysis.

The rate at which respiratory competent yeast catabolize glucose depends on the availability of oxygen. This phenomenon is known as the Pasteur effect (Krebs, 1972; Racker, 1974; Ramaiah, 1974). Our previous studies of respiratory competent *Saccharomyces cerevisiae* have shown an approximately 2-fold reduction in the rate of glucose utilization upon oxygenation (den Hollander et al., 1986a,b) in agreement with some earlier results (Stickland, 1956).

In order to investigate the enzymatic basis of the Pasteur effect, a series of studies have recently been completed in this laboratory. In one of the studies (den Hollander et al., 1986a), the in vivo flow through phosphofructokinase (PFK) was measured under anaerobic and aerobic conditions in acetate-grown cells that were harvested at mid-log phase. The net glycolytic flow through the Embden–Meyerhof–Parnas pathway was determined by first measuring the overall glucose utilization rate and then correcting for glucose consumption by nonglycolytic pathways. The overall glucose utilization rate was determined by measuring the time course of [1-^{13}C]glucose consumption by ^{13}C NMR.[1] Nonglycolytic flows such as trehalose biosynthesis, glycogen biosynthesis, and the phosphogluconate pathway were evaluated by additional ^{13}C NMR studies using labeled glucose and with previous data obtained from ^{14}C radioisotopic determinations of the different end products of ^{14}C glucose metabolism. The net glycolytic flux determined by these measurements equals the unidirectional PFK flow, providing that the reverse flow through Fru-1,6-P_2ase is negligible. Little attention has previously been directed to contributions from Fru-1,6-P_2ase activity in the kinetic control of glycolysis since this enzyme is subject to catabolite inactivation in the presence of glucose (Tortora, 1981; Lenz, 1981; Gancedo, 1971). However, in experiments using [6-^{13}C]glucose, analysis of the label distribution in trehalose indicated that the Fru-1,6-P_2ase activity is not totally inactivated on a short time scale (within 20 min) under aerobic conditions. In fact, its flux was ~40% that of the forward direction (den Hollander et al., 1986a).

In a parallel study, the intracellular concentrations of known allosteric effectors of PFK were determined by ^{31}P NMR with the aid of chemical analysis under both anaerobic and aerobic conditions. These concentrations were established in vitro so as to mimic the intracellular conditions found in vivo (Reibstein et al., 1986). The in vitro preparations reproduced the measured in vivo rate of PFK and determined the sensitivity of the PFK rate to the various individual effectors. These studies demonstrated that the change in PFK activity upon oxygenation cannot be ascribed entirely to changes in any one particular effector, but rather to contributions from a variety of effectors, with fructose 2,6-bisphosphate and the substrate fructose 6-phosphate dominating.

In addition to PFK, other enzymes have been implicated in the observed modulation of glycolytic rate. Previous ^{31}P and ^{13}C NMR studies performed in this laboratory have shown that glycolytic control exists at the glucose uptake step by either hexokinase and/or glucose transport (den Hollander et al., 1986a). The existence of an oppositely directed flow through Fru-1,6-P_2ase under aerobic conditions (on a short time scale), as mentioned above, demonstrates that futile cycling occurs and corresponds to a potential long-term control point. In addition, the accumulation of the PFK end product, Fru-1,6-P_2, at concentrations well above the K_m for aldolase, indicated that a control point also exists below PFK.

In the present paper, ^{31}P NMR ST studies have been used to accumulate more kinetic information regarding flows through the hexose part of the Embden–Meyerhof–Parnas pathway under conditions where the Pasteur effect is observed in yeast. In these ST experiments, a nonequilibrium magnetization is introduced into the ATP_γ phosphate peak and its

† This work was supported by National Institutes of Health Grant AM 27121.

* Address correspondence to this author at the Department of Biochemistry, Brandeis University, Waltham, MA 02254.

‡ Present address: Philips Medical Systems, 5600 MD Eindhoven, The Netherlands.

[1] Abbreviations: NMR, nuclear magnetic resonance; ST, saturation transfer; ATP, adenosine 5′-triphosphate; PME, phosphomonoester; NTP, nucleoside triphosphate.

0006-2960/87/0426-7493$01.50/0

transfer to the phosphate resonances of G6P and [1-P]Fru-1,6-P_2 by the hexokinase and phosphofructokinase reactions, respectively, is monitored. The steady-state reduction in the PME magnetization provides information regarding flows through these metabolites. A complicating factor in the analysis of the ST data is that the phosphomonoester peak in our yeast suspensions contains unresolved signals from three glycolytic intermediates, G6P, F6P, and Fru-1,6-P_2, which may all contribute to the saturation transfer. Furthermore, the sugar phosphate metabolites maintain nonequilibrium steady-state concentrations by setting up a multiple-exchange network. In a simple two-site equilibrium process, ST determination of unidirectional rates is fairly straightforward. However, for the multiple-site exchange case, additional flow must be considered as discussed by Ugurbil et al. (1985). Interpretation of the ST results was made possible by conducting ^{13}C NMR studies similar to those performed earlier in acetate-grown mid-log yeast by den Hollander et al. (1986a) and by quantitating the concentrations of the PME metabolites in acid extracts with ^{31}P NMR. These additional measurements were used to derive a model and several flux relationships that permitted ST determination of the unidirectional flows into and out of G6P and Fru-1,6-P_2.

Experimental Procedures

Cell Growth. The *Saccharomyces cerevisiae* strain NCYC 239 was grown aerobically for 24 h at 30 °C to stationary phase in a liquid medium containing 2% bactopeptone, 1% yeast extract, and 2% glucose. The cultures were cooled on ice and then harvested by low-speed centrifugation at 4 °C. The cells were washed twice in ice-cold buffer containing 5 mM KH_2PO_4, 0.86 mM K_2HPO_4, 2 mM $MgSO_4$, 1.7 mM NaCl, and 50 mM 2-(*N*-Morpholino)ethanesulfonic acid (MES) adjusted to pH 6.0 by using NaOH. In ^{13}C NMR experiments, 50 mM $Na_2H_2P_2O_7$ was substituted for MES. Cell suspensions were prepared and examined by NMR at densities of 10% and 40% wet weight.

NMR Experimental Conditions. Glucose was added to 15 mL of the cell suspension in a 20-mm NMR tube. A double-bubbler apparatus was inserted (Gillies et al., 1982), and the suspension was bubbled with either oxygen or nitrogen. Gas delivery rates corresponding to 1300 mL/min (upper bubbler) and 50 mL/min (lower bubbler) with 95% N_2/5% CO_2 were used for anaerobic experiments and rates of 1700 mL/min (upper bubbler) and 170 mL/min (lower bubbler) with 95% O_2/5% CO_2 were used for aerobic experiments. Gas delivery rates that ensured O_2 saturation of the cell suspension during aerobic NMR experiments were determined by monitoring the dissolved oxygen concentration using a Yellow Springs oxygen electrode in an apparatus similar to that used for NMR experiments.

In Vivo ^{13}C NMR Spectroscopy. ^{13}C NMR spectra were acquired by using a Bruker WH 360 WB spectrometer operating at 90.55 MHz. [1-^{13}C]- and [6-^{13}C]glucose additions to 15 mL of a 10% cell suspension were monitored with time by ^{13}C NMR. Experiments were also performed with 2.0 g of unlabeled glucose. Spectra were obtained with a 45° pulse and a 2-s repetition rate by using the MLEV pulse sequence (Levitt et al., 1983) to decouple protons. Gated decoupling was employed to suppress nuclear Overhauser enhancement using a decoupling power of 2 W. No decoupler heating was observed throughout the measurements. Glucose utilization rates were determined from the slope of a graph of combined natural abundance or labeled $C_{1\alpha}$ and $C_{1\beta}$ glucose signals versus time. Glucose concentrations were determined by extrapolation of the slope to zero time.

In Vivo ^{31}P NMR Saturation Transfer. ^{31}P NMR spectra were obtained at 145.78 MHz. A frequency synthesizer driving an auxillary amplifier generated the radio frequency (rf) field used for saturating the NTP_γ resonance in both T_1 and ST experiments. A 68° pulse and a 2.6-s relaxation delay were used for saturation-transfer experiments. The PME peak is fully relaxed under these pulsing conditions. The saturation frequency was centered alternately at the ATP_γ signal and at a control point equidistant to the low-field side of the PME resonance every 70 s (24 scans). Data were collected in files of 144 scans. Alteration of the rf field between control and ATP_γ positions helped to reduce errors in the spectra resulting from small variations in metabolite levels with time and from direct saturation effects. Inversion recovery experiments were performed in the presence of a saturating rf field at NTP_γ by using a 180°–*t*–90° pulse sequence in which *t* was varied between 0.05 and 6 s. Slopes obtained from these recovery curves provide apparent longitudinal (T_{1iapp}) relaxation times (Mann, 1977).

The areas of the control and PME difference peaks were determined by cutting out and weighing peaks in addition to using the Bruker integration routine. The concentration of metabolites contained within the PME resonance was calculated by measuring the total PME integral in vivo and comparing it to the standarized methyl phosphonate integral. Individual concentrations were then determined from the relative signal intensities of G6P, Fru-1,6-P_2, F6P, and α-GP measured in acid extract spectra. To convert relative to absolute concentrations it was assumed that 1.67 g of wet yeast contain 1 mL of cell water (Gancedo & Gancedo, 1973).

Acid Extracts. Acid extracts were prepared as previously described (den Hollander et al., 1986). For ^{13}C spectra, 3 mL of the acid extract was placed in a 10-mm NMR tube, and the spectra were acquired by using a pulse interval of 7.5 s and a flip angle of 45°. Decoupling of protons was employed only during acquisition to suppress Overhauser enhancement, using a decoupling power of 8 W. The fully relaxed ^{31}P NMR acid extract spectra were obtained by using a 45° pulse and 7.5-s relaxation delay. A power of 2 W was used to decouple protons.

O_2 Consumption Measurements. To verify that the cell suspension remained respiratory competent throughout aerobic NMR experiments, oxygen consumption rates were monitored with a Yellow Spring oxygen electrode contained in a Model 53 Yellow Spring bath stirrer assembly unit at 25 °C. Aliquots were taken from NMR samples throughout the experiment, diluted to 1% in oxygenated buffer, and oxygenated further for 10 min before the measurement was conducted. Rates were determined from the slope of a plot of O_2 concentration versus time.

Results

^{31}P NMR Saturation-Transfer Studies. The saturation transfer (control) M^0 spectra of aerobic and anaerobic glucose-fed cells are shown in Figure 1a. The spectra were acquired with the saturating rf field positioned downfield from the PME resonance at ~16.5 ppm. In alternate spectra (M), the rf field was centered at −5.0 ppm (Figure 1b) to saturate the NTP_γ resonance. The difference spectra shown in Figure 1c were obtained by subtracting the spectra in which NTP_γ was saturated from the control (M^0) spectra. The PME peaks were affected by saturation of NTP_γ under both anaerobic and aerobic conditions as illustrated by the difference peaks in Figure 1c.

The fractional change in the PME magnetization during saturation of the NTP_γ resonance ($\Delta M/M^0$) under anaerobic

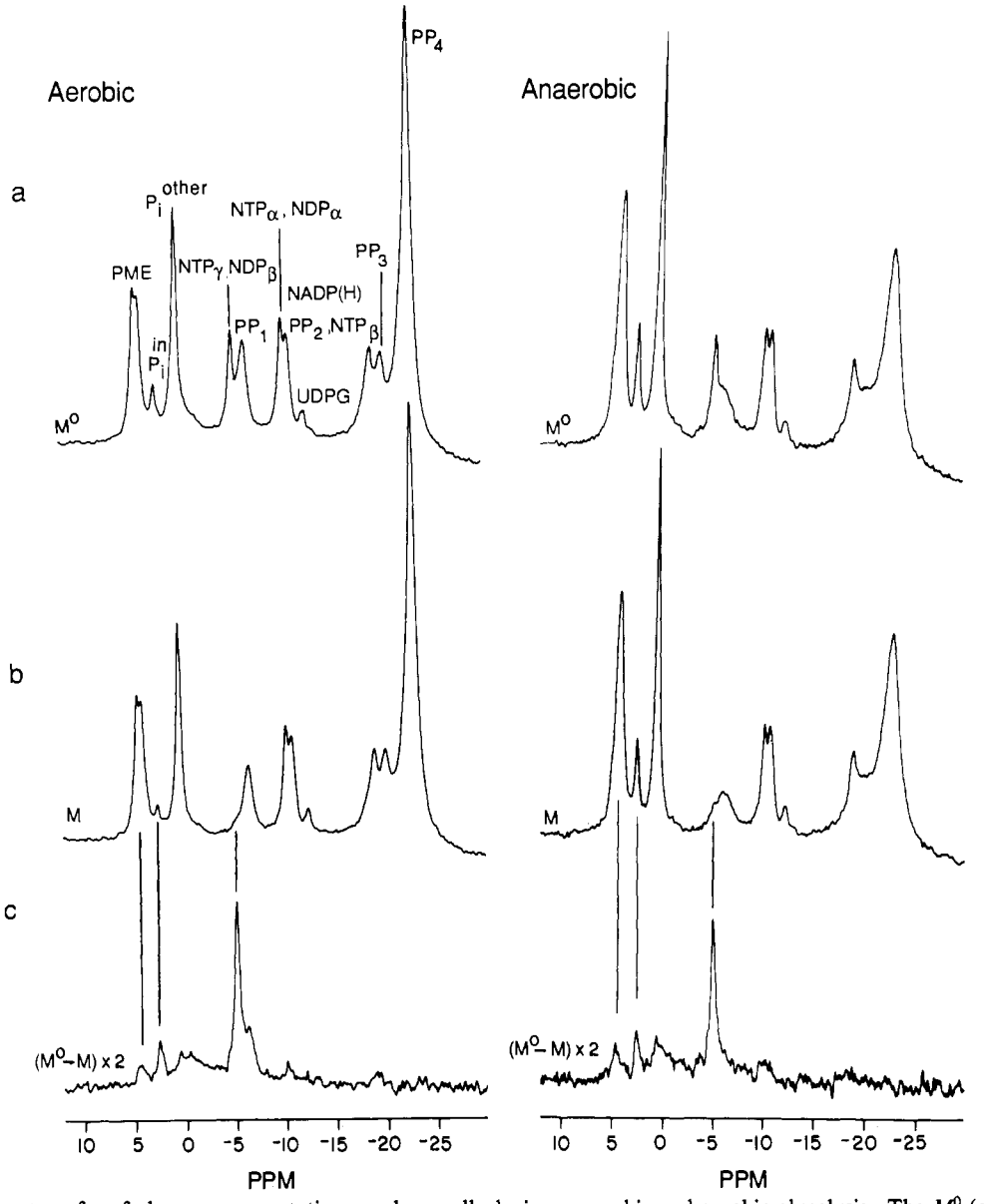

FIGURE 1: Saturation transfer of glucose-grown stationary phase cells during anaerobic and aerobic glycolysis. The M^0 (a, control) and M (b, ATP saturated) spectra were obtained as described in the text. (c) Difference (ΔM) spectra.

conditions was quantitated and averaged over five experiments to obtain a value of 0.04 ± 0.01. An apparent T_1 PME value of 0.9 ± 0.1 s was determined from an inversion recovery experiment performed during steady-state saturation of the NTP_γ peak. The error was estimated by using a least-squares linear regression program. In aerobic cell suspensions supplied with glucose, a $\Delta M/M^0$ value of 0.04 ± 0.01 (n = 4) was obtained. The data are listed in Table II.

The PME resonance consists predominately of G6P, Fru-1,6-P_2, F6P, and α-glycerol phosphate (den Hollander et al., 1981, 1986b). Resonances from these metabolites were resolved in ^{31}P spectra of acid extracts with metabolite concentrations quantitated (Table I) as described under Experimental Procedures. General inspection of Table I reveals that the G6P concentration is significantly higher and the concentration of α-glycerol phosphate (α-GP) lower under aerobic conditions relative to those under anaerobic conditions.

^{13}C NMR Studies. Glucose consumption rates were measured by adding [1-^{13}C]glucose or natural abundance glucose to the cell suspensions and then monitoring the C_1 glucose α and β anomer signals as a function of time with ^{13}C NMR. The measured glucose consumption rates at various initial glucose concentrations are listed in Table III. The anaerobic glucose consumption rate is approximately 2-fold higher than the aerobic rate. These rates agree with the glucose consumption rates previously determined in respiratory competent yeast (den Hollander et al., 1986a,b). In all experiments, glucose consumption rates were observed to be independent of glucose concentration.

Table I: Phosphomonoester Metabolite Concentrations

metabolite	fraction of PME peak		concn (μmol/g of wet cells)	
	anaerobic	aerobic	anaerobic	aerobic
fructose 1,6-bisphosphate[a]	0.70 ± 0.02[c]	0.66 ± 0.02	3.4	2.2
glucose 6-phosphate	0.07 ± 0.01	0.15 ± 0.01	0.7	1.1
fructose 6-phosphate[b]	0.02	0.05	0.2	0.4
α-glycerol phosphate	0.21 ± 0.02	0.09 ± 0.01	2.0	0.6
other		0.05 ± 0.01		

[a] Note that Fru-1,6-P_2 contains resonances from both phosphates. [b] Derived from G6P concentration by assuming that glucose-6-phosphate isomerase is in equilibrium (Johnson, 1960) with [F6P] = 1/3-[G6P]. [c] Standard deviation. Determined from a total of four experiments.

Table II: Saturation-Transfer Results

conditions	$\Delta M/M^0_T$	app T_1 PME (s)		app rate constant[a] (s^{-1}) lower	app rate constant[a] (s^{-1}) upper		flux [μmol min^{-1} (g of wet cells)$^{-1}$] lower[b]	flux [μmol min^{-1} (g of wet cells)$^{-1}$] upper[c]
anaerobic	0.04 ± 0.01	0.9 ± 0.1				V_1	14.2 ± 4.3	11.6 ± 5.0
			k_2	0.05	0.12	V_2	2.6 ± 0.8	6.5 ± 2.0
			k_3	0.21	0.18	V_3	11.6 ± 3.5	10.0 ± 3.0
			k_4	0.06	0.05	V_4	11.6 ± 3.5	10.0 ± 3.0
aerobic	0.04 ± 0.01					V_1	8.9 ± 2.7	10.3 ± 3.1
			k_2	0.02	0.05	V_2	2.3 ± 0.7	4.8 ± 1.4
			k_3	0.10	0.09	V_3	8.6 ± 2.6	7.8 ± 2.3
			k_{-3}	0.02	0.02	V_{-3}	2.0 ± 0.6	2.3 ± 0.7
			k_4	0.05	0.04	V_4	6.6 ± 2.0	5.5 ± 1.6

[a] Measured from saturation transfer and T_1 experiments. [b] Fluxes evaluated relative to lower limit of 8% glucose catabolized by the phosphogluconate pathway. [c] Fluxes evaluated relative to upper limit of 29% glucose catabolized by the phosphogluconate pathway.

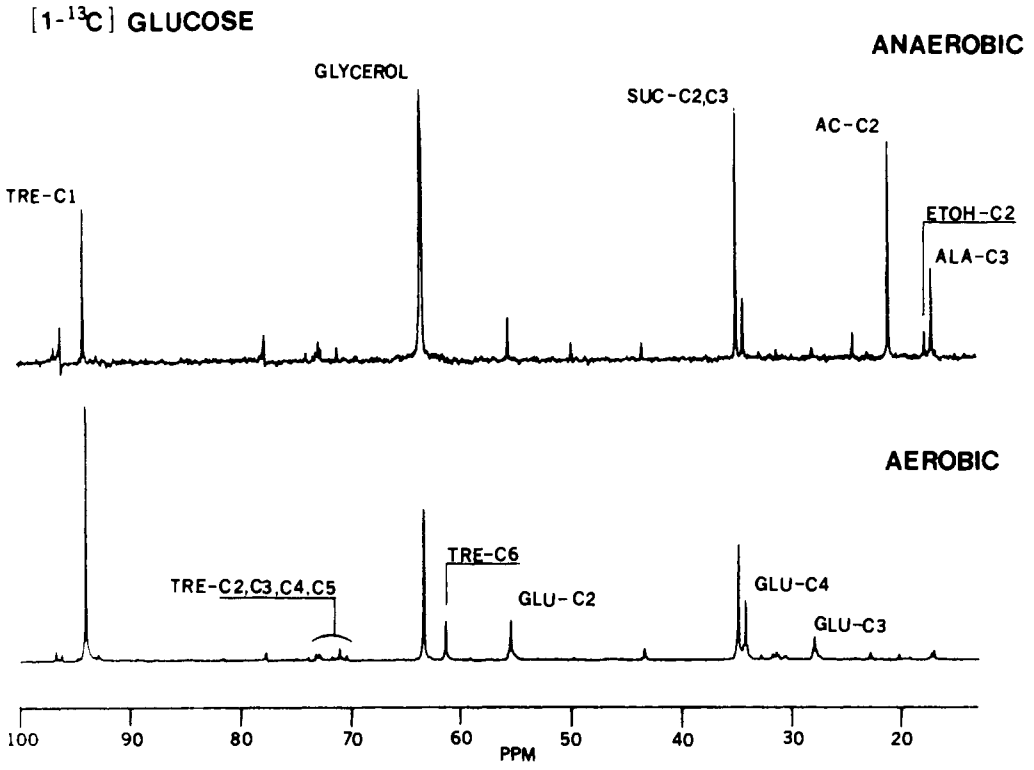

FIGURE 2: ^{13}C NMR spectra of acid extracts taken approximately 45 min after [1-^{13}C]glucose addition to a 10% cell suspension. The upper trace shows the extract spectrum obtained under aerobic conditions, while the lower trace is of the anaerobic extract. Aerobically, the ratio of C_6/C_1 is 0.13, whereas no detectable C_6 trehalose resonance is observed under anaerobic conditions.

We have also conducted experiments with 6-^{13}C-enriched glucose, similar to earlier studies performed in this lab, to estimate the amount of futile cycling between PFK and Fru-1,6-P_2ase in glucose-grown derepressed cells. It has previously been shown (den Hollander et al., 1986b) in experiments with [6-^{13}C]glucose that the label from C_6 glucose was scrambled between the C_1 and C_6 positions of Fru-1,6-P_2 by rapid flows through aldolase and triose-phosphate isomerase (TPI). The degree of this scrambling was measured by comparing the intensities of the C_1 and C_6 Fru-1,6-P_2 peaks in extracts. Once this scrambling was measured, the relative label distribution in trehalose C_1 and C_6 carbons was used to calculate the back flux from Fru-1,6-P_2 to F6P via Fru-1,6-P_2ase by the equation

$$V_1/V_{-3} = f_1(1/r_{16} - 1/R_{61}) \quad (1)$$

In this expression, V_1 is the rate of glucose conversion to G6P, V_{-3} is the rate of hydrolysis of Fru-1,6-P_2, and f_1 is the fraction of the Fru-1,6-P_2 C_1 carbon labeled during an experiment with [6-^{13}C]glucose. The ratio of ^{13}C label observed in the C_1 and C_6 carbons (C_1/C_6) of trehalose is r_{16}, while the corresponding ratio for Fru-1,6-P_2 is R_{61}. Possible contributions from transaldolase can be assessed by comparing r_{16} values when [1-^{13}C]glucose is supplied to the cells to its value during [6-^{13}C]glucose addition since transaldolase action cannot move the label from C_6 to C_1 in experiments with [6-^{13}C]glucose.

In our experiments, [1-^{13}C]glucose was supplied to yeast and monitored by ^{13}C NMR. The cells were acid extracted when the glucose levels were low, so that glucose signals did not interfere with quantitation of trehalose peaks. The trehalose C_6/C_1 ratio was quantitated in acid extract spectra by ^{13}C NMR since the ratio could not be measured reliably in vivo. The anaerobic and aerobic extract spectra are shown in Figure 2. The ^{13}C spectrum obtained from extracts of aerobic cells shows signals from carbon-labeled trehalose and glycerol, as well as glutamate, indicative of oxidative metabolism (den Hollander et al., 1986a,b). The trehalose resonances are labeled in both the C_1 and C_6 positions. The C_6/C_1 ratio was measured after correction for natural abundance trehalose ($C_{2,3,4,5}$) in three experiments to obtain an average C_6/C_1 value of 0.13 ± 0.03. However, a trehalose C_6 resonance was not detected in acid extract spectra taken from anaerobic cells. The absence of a detectable trehalose C_6 resonance indicates negligable flow through Fru-1,6-P_2ase since the amplitude of the trehalose C_1 resonance was large enough

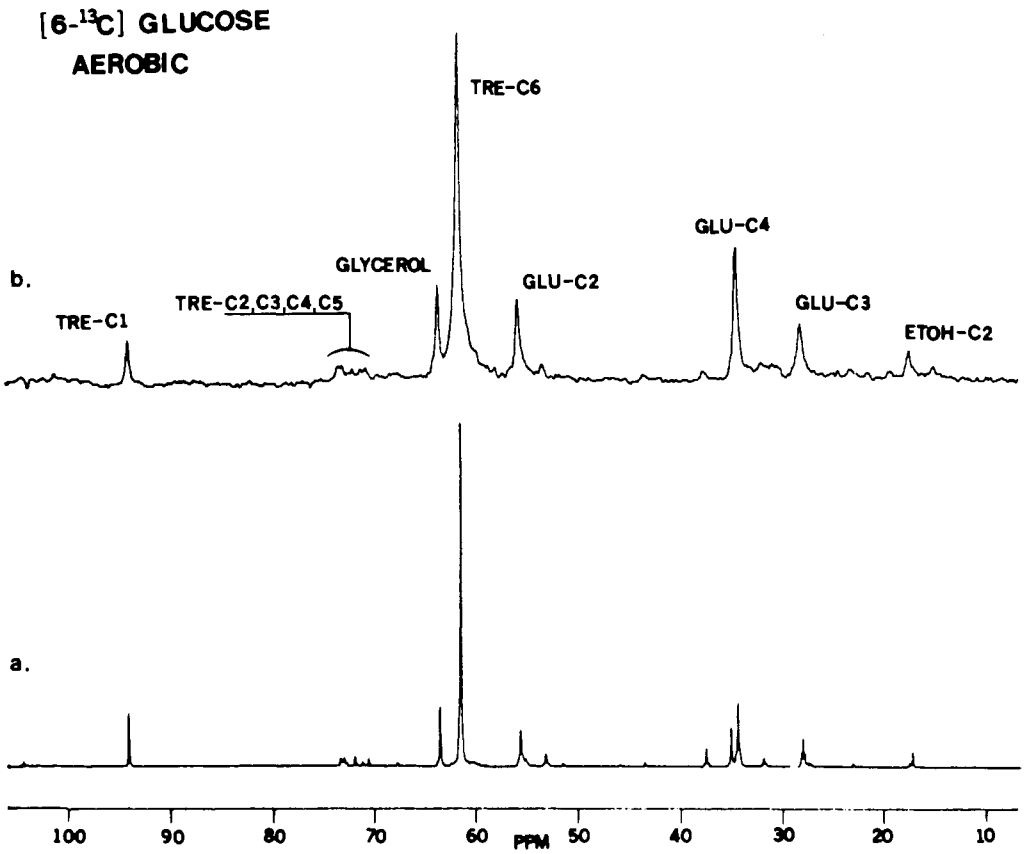

FIGURE 3: ^{13}C NMR spectra of glucose-grown derepressed cells supplied with [6-^{13}C]glucose under aerobic conditions. The lower trace gives the ^{13}C NMR spectrum of an acid extract prepared after aerobic catabolism of [6-^{13}C]glucose. The upper trace shows the ^{13}C NMR spectrum obtained in vivo approximately 45 min after the addition of [6-^{13}C]glucose. The C_1/C_6 trehalose is similar in both the in vivo and extract spectra. Data acquisition and sample conditions are described in the text.

Table III: Glucose Consumption Rates

conditions	glucose concn (μmol/g of wet cells)	glucose consumption rate [μmol min^{-1} (g of wet cells)$^{-1}$]
aerobic	6.29. × 10^2 [a]	8.2 ± 0.2
aerobic	6.29 × 10^2 [a]	8.7 ± 0.2
aerobic	5.55 × 10^2 [a]	8.5 ± 0.1
aerobic	1.85 × 10^3	8.3 ± 0.6
		av 8.4 ± 0.2
anaerobic	1.0m × 10^3 [a]	16.8 ± 0.2
anaerobic	1.07 × 10^3 [a]	15.4 ± 0.3
anaerobic	1.57 × 10^3	16.0 ± 0.5
anaerobic	1.85 × 10^3	15.9 ± 2.4
		av 16.0 ± 0.8

[a] Studies conducted with 99% ^{13}C-enriched glucose.

in these anaerobic extracts to detect a C_6 trehalose resonance an order of magnitude smaller.

Experiments were also performed on aerobic cells supplied [6-^{13}C]glucose, and the label distribution in trehalose was determined both in acid extract spectra and in vivo by ^{13}C NMR. The spectra are shown in Figure 3. A C_1 trehalose signal was observed both in the intact cell and in acid extracts with a C_1/C_6 ratio of 0.10 ± 0.02 (n = 2). No significant variation in the C_1/C_6 value was observed throughout these experiments (90 min), indicating that the Fru-1,6-P_2ase flux (V_{-3}) was not changing over time. Spectra acquired from experiments using [1-^{13}C]- and [6-^{13}C]glucose under aerobic conditions show a similar degree of label scrambling, indicating that most of the scrambling was caused by aldolase and TPI. In previous experiments using [6-^{13}C]glucose, the Fru-1,6-P_2 C_1/C_6 ratio was observed to be close to unity (den Hollander et al., 1979). We have established an upper limit for f_1 by

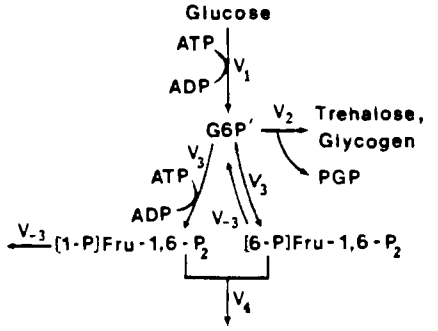

FIGURE 4: Kinetic scheme used for analysis of saturation-transfer data.

setting this value equal to 0.5 for complete scrambling of the label in Fru-1,6-P_2. A lower limit for V_{-3} corresponding to $0.22V_1$ was obtained by substituting $1/r_{16}$ into eq 1.

Discussion

The kinetic scheme in Figure 4 has been used for the analysis of ST data. All terms in this kinetic scheme describe unidirectional flows. In both models, k_1(glucose) = V_1 represents the rate of glucose phosphorylation. The flow out of G6P into the phosphogluconate pathway in addition to trehalose and glycogen pools is denoted by $V_2 = K_2$[G6P']. In this expression, G6P and F6P have been combined into one pool (G6P') since phosphoglucoisomerase is much faster (Johnson, 1960) than the net flux through the glycolytic pathway. $V_3 = k_3$[G6P'] corresponds to the unidirectional flow through PFK, and $V_{-3} = k_3$[Fru-1,6-P_2] is the fructose 1,6-bisphosphatase flux. We have designated the net flow out of Fru-1,6-P_2 to be equal to $V_4 = k_4$[Fru-1,6-P_2] for the following reasons. Previous studies performed by den Hollander et al.

(1979) have shown that flows through aldolase and TPI are near equilibrium, so that Fru-1,6-P_2, glyceraldehyde 3-phosphate, and dihydroxyacetone phosphate constitute one pool. This pool can be approximated by Fru-1,6-P_2 as dihydroxyacetone phosphate and glyceraldehyde 3-phosphate concentrations are much lower than that of Fru-1,6-P_2. If a unidirectional flow through glyceraldehyde-3-phosphate dehydrogenase/phosphoglycerate kinase is assumed to occur (Campbell-Burk et al., 1987), the flow out of Fru-1,6-P_2 is k_4[Fru-1,6-P_2].

In these saturation-transfer experiments, the ATP γ-phosphate resonance is saturated with an rf field and the steady-state magnetization of the PME resonance, which contains the unresolved resonances of F6P, G6P, Fru-1,6-P_2, and α-GP, is measured after a steady state in PME magnetization is achieved.

Fru-1,6-P_2 gives rise to two separate ^{31}P resonances. The ^{31}P nuclear labeling scheme differentiates [1-P]Fru-1,6-P_2 from [6-P]Fru-1,6-P_2 since saturation of ATP_γ selectively labels [1-P]Fru-1,6-P_2 by PFK and not [6-P]Fru-1,6-P_2. A nuclear spin-label appears in [6-P]Fru-1,6-P_2 indirectly as a result of flow from labeled G6P′ (V_3) and by action of aldolase and triose-phosphate isomerase due to scrambling from [1-P]-Fru-1,6-P_2.

The Bloch equations, which quantitatively describe the spin magnetization of G6P and Fru-1,6-P_2 in the presence of the exchange reactions shown in Figure 4, are listed in eq 2–4. For simplicity of notation let G6P′ = (F6P + G6P) = a, [1-P]Fru-1,6-P_2 = b, and [6-P]Fru-1,6-P_2 = c.

$$dM_a/dt = (M^0_a - M_a)(1/T_{1a}) - (k_2 + k_3)M_a + k_1M_{ATP\gamma} + k_{-3}M_c \quad (2)$$

$$dM_b/dt = (M^0_b - M_b)(1/T_{1b}) - (k_4 + k_{-3})M_b + k_3M_{ATP\gamma} \quad (3)$$

$$dM_c/dt = (M^0_c - M_c)(1/T_{1c}) - (k_4 + k_{-3})M_c + k_3M_a \quad (4)$$

In these equations M^0 denotes the equilibrium magnetization of these metabolites, M is the magnetization at time t, and $1/T_1$ is the spin–lattice relaxation rate in the absence of exchange. Saturation of the γ-phosphate of ATP equalizes the Boltzmann populations so that no net transitions occur and $M_{ATP\gamma} = 0$. If the levels of G6P, F6P, and Fru-1,6-P_2 are in kinetic steady state and the signals are measured when the nuclear spin-label has reached steady state, then $dM_{a,b,c}/dt = 0$. The Bloch equations can be solved in terms of the fractional change in each metabolite magnetization, $\Delta M/M^0 = M^0 - M/M^0$.

$$\Delta M/M^0_a = (k_2 + k_3)/(1/T_{1a} + k_2 + k_3) - k_{-3}M_c/(1/T_{1a} + k_2 + k_3)M^0_a \quad (5)$$

$$\Delta M/M^0_b = (k_{-3} + k_4)/(1/T_{1b} + k_{-3} + k_4) \quad (6)$$

$$\Delta M/M^0_c = (k_{-3} + k_4)/(1/T_{1c} + k_{-3} + k_4) - k_3M_a/(1/T_{1c} + k_{-3} + k_4)M^0_c \quad (7)$$

General inspection of Figure 4 reveals that G6P′ and Fru-1,6-P_2 are maintained at steady state by multiple flows. It is not possible to reduce this multiple-site exchange problem into a two-site exchange by the double-irradiation method described by Ugurbil et al. (1985) since the F6P, G6P, [1-P]Fru-1,6-P_2, and [6-P]Fru-1,6-P_2 signals are not resolved in vivo. Therefore, we have quantitated the unidirectional flows through PFK and the Fru-1,6-P_2ase flow under anaerobic and aerobic conditions using the following equation for the total $\Delta M/M^0_T$:

$$\Delta M/M^0_T = (\Delta M/M^0)_a(M^0_a/M^0_T) + (\Delta M/M^0)_b(M^0_b/M^0_T) + (\Delta M/M^0)_c(M^0_c/M^0_T) \quad (8)$$

The $(M^0/M^0_T)_{a,b,c}$ terms denote the fraction of components a, b, and c in the PME peak. These values along with the PME metabolite concentrations are listed in Table I. Equation 8 does not contain an expression for α-GP for the following reasons. For a nuclear "spin-label" to appear in α-GP, the glycerol kinase catalyzed reaction must have a time constant similar to the longitudinal relaxation rate for α-GP, which is approximately 1 s^{-1}. Gancedo et al. (1968) showed *S. cerevisiae* to be relatively impermeable to glycerol. The low growth of *S. cerevisiae* on glycerol has been correlated to low specific activity of glycerol kinase, as some strains use it aerobically as the sole carbon source. The enzyme does not need glycerol for induction and is repressed by glucose (Sprague & Cronan, 1977). The maximal rate through this reaction has been estimated to be much lower than our measured glucose utilization rates under anaerobic and aerobic conditions (Gancedo et al., 1968). Moreover, a transfer was not observed in ST experiments performed on acetate-grown mid-log cells in which a much larger percentage of glycerol is formed (Campbell et al., 1985; den Hollander et al., 1986a).

Our ^{13}C NMR kinetic studies and previous radioisotope determinations have allowed evaluation of the fractional flow of glucose in the phosphogluconate pathway and in the biosynthesis of glycogen and trehalose, as well as the Fru-1,6-P_2ase flux. These data have been used to derive several flux relationships for ST determination of unidirectional flows into and out of G6P′ and Fru-1,6-P_2 as follows. The rate of glucose phosphorylation (V_1) was evaluated under anaerobic and aerobic conditions by monitoring the time course of glucose disappearance by ^{13}C NMR. The results are listed in Table III. The rate of Fru-1,6-P_2 conversion to F6P (V_{-3}) was determined from ^{13}C NMR label distribution studies and found to have a lower limit of $0.22V_1$ in aerobic cells. However, no flow was observed under anaerobic conditions. The percentage of total glucose stored in polysaccharides and trehalose has been determined (in this laboratory) previously to be 10.5% and 17.5% under anaerobic and aerobic conditions, respectively, in glucose-grown derepressed cells (den Hollander et al., 1986a). To determine the fraction of glucose utilized in nonglycolytic paths (V_2 in the kinetic scheme), phosphogluconate contributions have been estimated from previous measurements performed in this laboratory. Under anaerobic conditions, the percentage of glucose catabolized by the phosphogluconate pathway was determined by den Hollander et al. (1986a) and found to be 8% in glucose repressed cells and as much as 29% in acetate-grown derepressed cells. These values were determined by comparing formation of $^{14}CO_2$ from [1-^{14}C]glucose and from [6-^{14}C]glucose (Koshland & Westheimer, 1950; Beevers & Gibbs, 1954). It is more difficult to assess phosphogluconate contributions aerobically as CO_2 is also produced oxidatively by the tricarboxylic acid (TCA) cycle, although these contributions are expected to be at least equal to the anaerobic flow. Glucose metabolism in our glucose-grown derepressed cells is expected to be intermediate to that of glucose repressed and acetate-grown derepressed cells with respect to levels of glycolytic enzymes and the overall importance of the glycolytic pathway (den Hollander et al., 1981). Therefore, we would expect that between 8% and 29% of the total glucose is catabolized by the phosphogluconate pathway in glucose-grown derepressed cells.

This information has been used to express the nonglycolytic flows (V_2), the PFK flux (V_3), and the Fru-1,6-Pase flux (V_{-3}) in terms of V_1, the rate of glucose phosphorylation. These flux

Table IV

	anaerobic		aerobic	
	lower[a]	upper	lower	upper
$V_2 = k_2$[G6P^1]	$0.185V_1$	$0.395V_1$	$0.255V_1$	$0.465V_1$
$V_3 = k_3$[G6P^1]	$0.815V_1$	$0.605V_1$	$0.965V_1$	$0.755V_1$
$V_{-3} = k_{-3}$[Fru-1,6-P$_2$]			$0.22V_1$	$0.22V_1$
$V_4 = k_4$[Fru-1,6-P$_2$]	$0.815V$	$0.605V_1$	$0.74V_1$	$0.535V_1$

[a] Determined from upper and lower limits placed on the fraction of glucose catabolized by the phosphogluconate pathway.

relations are listed in Table IV.

ST-determined unidirectional flows (V_1, V_2, V_3, V_4) were evaluated under anaerobic conditions in the following manner. Results obtained from ^{13}C NMR label distribution studies in anaerobic glucose-fed cells indicate the Fru-1,6-P$_2$ase is inactivated. We have set k_{-3} equal to zero in eq 5–7. These equations along with $\Delta M/M^0_T$ from Table II and the $M^0_{a,b,c}/M^0_T$ values from Table I can be substituted into eq 8 to obtain the expression:

$$0.04 = 0.09(k_2 + k_3)/(1/T_{1a}') + 0.35k_4/(1/T_{1b}') + 0.35k_4/(1/T_{1c}') - 0.35k_3M_a/M^0_c(1/T_{1c}') \quad (9)$$

We have replaced M_a by $M^0_a - (k_2 + k_3)M^0_a/(1/T_{1a}')$ from eq 2 to obtain

$$0.04 = 0.09(k_2 + k_3)/(1/T_{1a}') + 0.35k_4/(1/T_{1b}') + 0.35k_4/(1/T_{1c}') - 0.35k_3M^0_a/M^0_c(1/T_{1c}') + 0.35(k_2 + k_3)k_3M^0_a/M^0_c(1/T_{1c}')(1/T_{1a}') \quad (10)$$

We have measured longitudinal PME relaxation times during steady-state ATP$_\gamma$ saturation. These measurements include longitudinal relaxation due to exchange reactions (Mann, 1977). According to Figure 4, the apparent longitudinal relaxation rates corresponding to G6P′ ($1/T_{1a}'$) and Fru-1,6-P$_2$ ($1/T_{1b}'$, $1/T_{1c}'$) under anaerobic conditions are listed in eq 11–13.

$$1/T_{1a}' = 1/T_{1a} + k_2 + k_3 \quad (11)$$

$$1/T_{1b}' = 1/T_{1b} + k_4 \quad (12)$$

$$1/T_{1c}' = 1/T_{1c} + k_4 \quad (13)$$

Our measured PME apparent longitudinal relaxation rate does not distinguish between individual T_1 components of the PME peak, i.e., $1/T_{1a,b,c}$. However, since Fru-1,6-P$_2$ constitutes 70% of the PME peak, the experimentally measured T_1 apparent value has been set equal to $1/T_{1b,c}' = 1.1$ s^{-1}. Moreover, we have assumed that the intrinsic relaxation times in the absence of exchange (T_1) for the sugar phosphate metabolites, G6P, F6P, [1-P]Fru-1,6-P$_2$, and [6-P]Fru-1,6-P$_2$, were equal. Our assumption is based on the similar chemical structure and correlation time of the phosphate metabolites. Thus, $1/T_{1b,c}' = 1/T_1 + k_4 = 1.1$ s^{-1}.

Under anaerobic conditions, the fraction of glucose used for the synthesis of trehalose and glycogen has been determined in a previous study to be $0.105V_1$. We have estimated the fraction of glucose catabolized by the phosphogluconate pathway to be between 0.08 and 0.29. In the previous determination of the net glycolytic flow by ^{13}C NMR and radioisotope measurements, den Hollander et al. (1986a) assumed that, overall, the correction for glucose catabolism via the phosphogluconate pathway is limited due to resynthesis of hexose phosphates from pentose phosphates. However, phosphogluconate contributions are significant in ST measurements (between 8% and 29%) since the spin-label introduced into G6P by saturating ATP$_\gamma$ will relax on the order of its spin–lattice relaxation time (which is approximately 1 s). We would expect the spin-label to relax before hexose phosphate regeneration with a lower limit for the fraction of glucose catabolized by nonglycolytic flows to be $0.185V_1 = k_2$[G6P′]. Under steady-state conditions, $V_3 = 0.815V_1 = k_2$[G6P′] and $V_4 = 0.815V_1 = $[Fru-1,6-P$_2$]. The apparent rate constants k_2, k_3, and k_4 can now be expressed in terms of V_1. The substitutions give $k_2 = 0.21V_1$, $k_3 = 0.91V_1$, and $k_4 = 0.24V_1$. The $1/T_{1a}'$ value $= 1/T_1 + k_2 + k_3$ has been determined to be $1.1 \pm 0.87V_1$ by substituting $1/T_1$ into the expression for $1/T_{1b,c}$ and expressing apparent rate constants k_2 and k_3 in terms of V_1. The apparent rate constants and apparent longitudinal relaxation rates (eq 11–13) have been substituted into eq 10 and solved for V_1. The net glycolytic flow and the PFK flow were then determined with the values in Table II. Similarly, we have also determined the upper limit of these fluxes with the phosphogluconate pathway accounting for 29% of V_1 using the steady-state flux relationships in Table IV.

Aerobic fluxes through PFK and Fru-1,6-P$_2$ase can now be solved in a similar fashion with the inclusion of k_{-3} since the back flow is not negligible. The $\Delta M/M^0_T$ value of 0.04 and the fractional distribution of Fru-1,6-P$_2$, F6P, and G6P ($M^0_{a,b,c}/M^0_T$) in Table I were used to obtain eq 14. Aerobically, an additional unknown, M_c, is present in eq 14 since a unidirectional flow through Fru-1,6-P$_2$ase was observed (k_{-3} is nonzero). Expressions for M_a and M_c were solved simultaneously and substituted into the above expression to obtain the expression

$$0.04 = 0.20(k_2 + k_3)/(1/T_{1a}') - 0.20k_{-3}M_c/(1/T_{1a}')M^0_a + 0.33(k_{-3} + k_4)/(1/T_{1b}') + 0.33(k_{-3} + k_4)/(1/T_{1c}') - 0.33k_3M_a/(1/T_{1c}')M^0_c \quad (14)$$

$$0.04 = 0.20(k_2 + k_3)/(1/T_{1a}') - 0.20(k_3) \times (1/T_{1c})M^0_c/M^0_a(1/T_{1a}')(1/T_{1c}') + 0.33(k_{-3} + k_4)/(1/T_{1b}') + 0.33(k_{-3} + k_4)/(1/T_{1c}') - 0.33k_3(1/T_{1a})M^0_a/M^0_c(1/T_{1c}')(1/T_{1a}') \quad (15)$$

Under aerobic conditions, V_{-3} was determined to be $0.22V_1 = k_{-3}$[Fru-1,6-P$_2$] with a lower limit of V_2 corresponding to $0.255V_1 = k_3$[G6P′]. Therefore, under steady-state conditions, $V_3 = 0.965V_1 = $[G6P′] and $V_4 = 0.745V_1 = $[Fru-1,6-P$_2$]. The apparent rate constants can be expressed in terms of V_1 to obtain $k_2 = 0.17V_1$, $k_3 = 0.64V_1$, $k_{-3} = 0.10V_1$, and $k_4 = 0.34V_1$. After substitution of these values into eq 15 and solving for V_1, the PFK (V_3), Fru-1,6-P$_2$ase, and net glycolytic flow ($V_3 - V_{-3}$) were determined with the values presented in Table II. The upper limits of these flows were determined in an analogous manner by using the flux relationships listed in Table IV.

We have placed upper and lower limits on our ST-determined fluxes based on estimates that between 8% (lower limit) and 29% (upper limit) glucose is catabolized by the phosphogluconate pathway in glucose-grown derepressed cells. The ST-measured value for V_1 was determined to have a lower limit of 14.2 ± 4.3 μmol min^{-1} (g of wet cells)$^{-1}$ and an upper limit of 16.5 ± 5.0 μmol min^{-1} (g of wet cells)$^{-1}$ under anaerobic conditions and lower and upper limits of 8.9 ± 2.7 and 10.3 ± 3.1 μmol min^{-1} (g of wet cells)$^{-1}$, respectively, under aerobic conditions. These values are similar to the ^{13}C NMR measured glucose consumption rate of 16.0 ± 0.8 and aerobic value of 8.4 ± 0.2 μmol min^{-1} (g of wet cells)$^{-1}$ (Table III). The ST-determined flow through PFK under anaerobic and aerobic conditions are listed in Table II. Under anaerobic conditions, the flow through PFK is equal to the net glycolytic flow, since our ^{13}C NMR label distribution measurements indicate that Fru-1,6-P$_2$ase is inactivated. Aerobically, the flow through Fru-1,6-P$_2$ase is approximately 20% of the PFK flow, indi-

cating that significant futile cycling takes place. Thus, the net glycolytic flow must be corrected for Fru-1,6-P_2ase to obtain the aerobic PFK flow. The combined PFK flux and the back flux through Fru-1,6-P_2ase during aerobic glycolysis gives rise to a net flux through the hexose part of the Embden–Meyerhof–Parnas pathway that is approximately 2-fold lower than the glycoytic flux during anaerobic glycolysis.

In this paper we have brought together data from ^{13}C NMR labeling experiments, measurements of intermediates by ^{31}P NMR, and ^{31}P ST NMR measurements and fit these results into a coherent picture. The ST experiments serve to confirm and strengthen data from the ^{13}C and ^{31}P NMR measurements of metabolites and end products.

References

Bannuelos, M., Gancedo, C., & Gancedo, J. M. (1977) *J. Biol. Chem. 252*, 6394–6398.

Beevers, H., & Gibbs, M. (1954) *Nature (London) 173*, 640–641.

Campbell, S. L., Jones, K. A., & Shulman, R. G. (1985) *FEBS Lett. 193*, 189–193.

Campbell-Burk, S. L., Jones, K. A., & Shulman, R. G. (1987) *Biochemistry* (preceding paper in this issue).

Den Hollander, J. A., Brown, T. R., Ugurbil, K., & Shulman, R. G. (1979) *Proc. Natl. Acad. Sci. U.S.A. 76*, 6096–6100.

Den Hollander, J. A., Ugurbil, K., Brown, T. R., & Shulman, R. G. (1981) *Biochemistry 20*, 5871–5880.

Den Hollander, J. A., Ugurbil, K., Brown, T. R., Bednar, M., Redfield, C., & Shulman, R. G. (1986a) *Biochemistry 25*, 203–211.

Den Hollander, J. A., Ugurbil, K., & Shulman, R. G. (1986b) *Biochemistry 25*, 212–219.

Gancedo, C. (1971) *J. Bacteriol. 107*, 401–405.

Gancedo, C., Gancedo, J.-M., & Sols, A. (1968) *Eur. J. Biochem. 5*, 165–172.

Gancedo, J.-M., & Gancedo, C. (1973) *Biochimie 55*, 205–211.

Gillies, R. J., Alger, J. R., den Hollander, J. A., & Shulman, R. G. (1982) in *Intracellular pH* (Nuccitelli, R., & Deamer, D. W., Eds.) pp 79–104, Alan R. Liss, New York.

Johnson, M. J. (1960) *Enzymes, 2nd Ed. 3*, 407–441.

Koshland, D. E., & Westheimer, F. H. (1950) *J. Am. Chem. Soc. 72*, 3383–3388.

Krebs, H. A. (1972) *Essays Biochem. 8*, 1–34.

Lagunas, R., & Gancedo, J. M. (1973) *Eur. J. Biochem. 37*, 90–94.

Lenz, A.-G., & Holzer, H. (1981) *FEBS Lett. 109*, 271–274.

Levitt, M. H., Freeman, R., & Frenkiel, T. (1983) in *Advances in Magnetic Resonance* (Waugh, J. S., Ed.) Vol. 2, pp 47–110, Academic, New York.

Mann, B. E. (1977) *J. Magn. Reson. 25*, 91–94.

Passonneau, J. V., & Lowry, O. H. (1962) *Biochem. Biophys. Res. Commun. 1*, 10–15.

Racker, E. (1974) *Mol. Cell. Biochem. 5*, 17–23.

Ramaiah, A. (1974) in *Current Topics in Cellular Regulation* (Horecker, B. L., & Stadtman, E. R., Eds.) Vol. 8, pp 297–345, Academic, New York.

Reibstein, D., den Hollander, J. A., Pilkis, S. J., & Shulman, R. G. (1986) *Biochemistry 25*, 219–227.

Sprague, G. F., Jr., & Cronan, J. E., Jr. (1977) *J. Bacteriol. 129*, 1335–1342.

Stickland, L. H. (1956) *Biochem. J. 64*, 498–515.

Tortora, P., Birtel, M., Lenz, A. G., & Holzer, H. (1981) *Biochem. Biophys. Res. Commun. 100*, 688–695.

Ugurbil, K., Petein, M., Maidan, R., Michurski, S., & From, A. H. L. (1986) *Biochemistry 25*, 100–107.